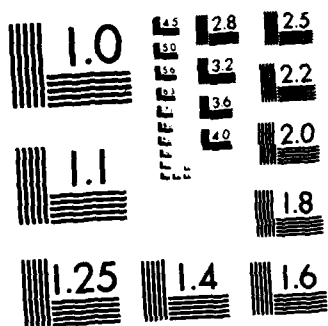


AD-A126 461 INVESTIGATION OF IMPURITY CONCENTRATIONS AND ELECTRICAL 1/1
PROPERTIES NEAR I..(U) UNIVERSITY OF SOUTHERN
CALIFORNIA LOS ANGELES DEPT OF MATERIALS D B WITTRY

UNCLASSIFIED 27 DEC 82 AFOSR-TR-83-0129 AFOSR-81-0094 F/G 20/12 NL

END
DATE
FILED
12-14-84
DTIC



MICROCOPY RESOLUTION TEST CHART
NATIONAL BUREAU OF STANDARDS-1963-A

WA A126461

SECURITY CLASSIFICATION UNCLASSIFIED REPORT DOCUMENTATION PAGE		READ INSTRUCTIONS BEFORE COMPLETING FORM
1. REPORT NUMBER AFOSR-TR- 83 - 0129	2. GOVT ACCESSION NO.	3. RECIPIENT'S CATALOG NUMBER
4. TITLE (and Subtitle) INVESTIGATION OF IMPURITY CONCENTRATIONS AND ELECTRICAL PROPERTIES NEAR INTERFACES		5. TYPE OF REPORT & PERIOD COVERED Final Report 2/1/81-8/31/82
6. AUTHOR(S) David E. Wittry		6. PERFORMING ORG. REPORT NUMBER
7. PERFORMING ORGANIZATION NAME AND ADDRESS University of Southern California Dept. of Materials Science Los Angeles, CA 90089-0241		10. PROGRAM ELEMENT, PROJECT, TASK AREA & WORK UNIT NUMBERS <i>61102F 2306/B1</i>
8. CONTRACT OR GRANT NUMBER(S) AFOSR-81-0094		12. REPORT DATE Dec. 27, 1982
9. CONTROLLING OFFICE NAME AND ADDRESS Air Force Office of Scientific Research Bolling Air Force Base Washington, DC 20332		13. NUMBER OF PAGES <i>18</i>
11. MONITORING AGENCY NAME & ADDRESS(if different from Controlling Office)		15. SECURITY CLASS. (of this report) UNCLASSIFIED
		15a. DECLASSIFICATION/DOWNGRADING SCHEDULE
16. DISTRIBUTION STATEMENT (of this Report) <i>Approved for public release; distribution unlimited.</i>		
17. DISTRIBUTION STATEMENT (of the abstract entered in Block 20, if different from Report)		
18. SUPPLEMENTARY NOTES		
19. KEY WORDS (Continue on reverse side if necessary and identify by block number) Secondary Ion Mass Spectrometry Photoluminescence Cathodoluminescence Gallium Arsenide		
20. ABSTRACT (Continue on reverse side if necessary and identify by block number) Studies of the nature of the thermal conversion on semi-insulating GaAs:Cr using photoluminescence, cathodoluminescence, and secondary ion mass spectrometry are described. Improvements in a quadrupole mass spectrometer instrument for secondary ion mass spectrometry are described and the applications of this instrument to significant problems in solid state electronics are discussed.		

INVESTIGATION OF IMPURITY CONCENTRATIONS AND
ELECTRICAL PROPERTIES NEAR INTERFACES

Final Technical Report

AFOSR Grant No. AFOSR-81-0094

February 1, 1981 - August 31, 1982

David B. Wittry

December 27, 1982

Abstract

Studies of the nature of the thermal conversion on semi-insulating GaAs:Cr using photoluminescence, cathodoluminescence, and secondary ion mass spectrometry are described. Improvements in a quadrupole mass spectrometer instrument for secondary ion mass spectrometry are described and the applications of this instrument to significant problems in solid state electronics are discussed.

Accession For	
NTIS GRAAI	<input checked="" type="checkbox"/>
DTIC TAB	<input type="checkbox"/>
Unannounced	<input type="checkbox"/>
Justification	
By _____	
Distribution/	
Availability Codes	
Dist	Avail and/or Special
A	



AIR FORCE OFFICE OF SCIENTIFIC RESEARCH (AFSC)
NOTICE OF APPROVAL FOR RELEASE TO DTIC
THIS REPORT HAS BEEN APPROVED FOR RELEASE TO DTIC.
MATTHEW J. WITTRY
Chief, Technical Information Division

1.0 Introduction

This research has been concerned principally with the problem of thermal conversion of GaAs:Cr, in which a low resistivity layer is formed on semi-insulating GaAs after heat treatment. Specimens of GaAs from Laser Diode Laboratories or Crystal Specialties, Inc. were heat treated at the Naval Ocean Systems Center (NOSC) using a tube furnace with flowing H₂ gas or at Hughes Research Laboratories using the Melt Controlled Ambient Technique (MCAT). These were studied by photoluminescence, cathodoluminescence and secondary ion mass spectrometry (SIMS).

In the course of this work a Quadrupole Mass Analyzer for Solids was placed in operation and computer programs were refined for obtaining depth profiles, mass-spectra histograms, and energy distributions of secondary ions.

2. Brief Description of the Work

2.1 Cathodoluminescence and photoluminescence

Low temperature cathodoluminescence spectra were obtained from fourteen specimens of GaAs including eight heat treated specimens. Before annealing, bands were observed at 1.509 eV and 1.23 eV. After annealing additional bands were observed at 1.496 eV, 1.363 eV, and 1.407 eV. The 1.363 band intensity was found to increase with increasing carrier concentration in the converted layer over three decades of intensity. This band was not observed in photoluminescence spectra; if it was present it was masked by the LO phonon replica of a very strong band with a peak at 1.41 eV. This latter peak was weak in the cathodoluminescence spectra compared with the 1.363 eV peak.

The difference in the photoluminescence spectra has been attributed to a difference in sampling depth for these two techniques. Based on this assumption and assuming that the diffusion constant for Ga vacancies is much larger than the diffusion constant for As vacancies, it is believed that the 1.363 peak is associated with recombination involving a Ga vacancy while the 1.41 eV peak is associated with an As vacancy. In addition, based on work published in the literature it is further proposed that the 1.363 eV involves Si on an As site paired with a Gallium vacancy and that this level is the acceptor level responsible for thermal conversion. A more detailed description of this work is given in a paper scheduled for publication in the January 1982 issue of J. Applied Physics (refer to Appendix A).

2.2 Secondary ion mass spectrometry

2.2.1 Results obtained with the Cameca IMS-3F

Secondary ion mass spectrometry (SIMS) results were obtained on six of the eight heat treated specimens and also on corresponding specimens that had not undergone heat-treatment. In all cases, the spectra from heat treated specimens 2 μm below the surface were identical to specimens not heat treated. Depth profiles of heat treated specimens all showed a shallow layer ($< .05 \mu\text{m}$) of high ^{52}Cr , ^{63}Cu and ^{28}Si and a thicker layer (1-2 μm) in which the ^{52}Cr concentration was lower than the bulk by \sim factor of 10. In all cases, the ^{28}Si ion intensity was comparable to or higher than the ^{52}Cr ion intensity. It was not known at the termination of the present grant whether this was due to interference from another species (e.g. $^{14}\text{N}_2$, $^{12}\text{C}^{16}\text{O}$, $^{27}\text{AlH}^+$, $^{12}\text{C}_2\text{H}_4^+$, $^{56}\text{Fe}^{++}$, etc.), or a high background due to the fact that the instrument had previously been used to run many specimens of silicon. However further

experiments are in progress to resolve this question.

2.2.2 Results obtained with the QMAS

Since the work on this grant began, efforts were being made to place into operation in our laboratory a quadrupole SIMS instrument made by Applied Research Laboratories called a Quadrupole Mass Analyzer for Solids (QMAS). However, it was only toward the end of the grant period that useful results were obtained. This was due partly to a) instrumentation problems (since this was a prototype instrument no instruction manual was available and all of the personnel who worked on this instrument were no longer at ARL) and partly to b) not being able to obtain graduate students qualified to debug this complex instrument. Toward the end of the grant period the hardware problems were under control, except for the primary beam current being too low to obtain satisfactory depth profiles. However, this was solved by devising a new bias circuit for the duoplasmatron.

In the course of evaluating the software that had been written for this instrument, a number of faults were discovered, for example, the program to calibrate the mass scale was not sufficiently accurate to provide a good fit over a large range of mass numbers.

Since a considerable fraction of the time spent on this project was devoted to the QMAS, it seems appropriate to include some results obtained up to now with this instrument. These are given in figures 1 - 8 (refer to Appendix B). The examples given show results obtained with three principal programs, namely i) a program for depth profiling multiple elements (Figs. 1 and 2); ii) a program for obtaining mass spectra plots in histogram form (Figs. 3 and 4); and iii) a program for obtaining the energy distribution of secondary ions (Figs. 5-8).

Figure 1 shows a depth profile of a superlattice consisting of alternating layers of Si and Si-7.5% Ge. This test specimen was grown at Rockwell using a MOCVD process. Figure 2 shows the depth distribution of Si implanted into GaAs. These results show that the many problems of obtaining depth profiles have been overcome (adequate ion intensities, good electronic aperturing, flat-bottom crater, etc.).

Figure 3 shows a histogram plot of a mass spectrum from Czochralski-grown silicon and figure 4 shows a histogram plot of a mass spectrum from GaAs. These plots incorporate automatic change from digital recording to analog recording at high count rates, a modification made by us. They also employ a modified calibration program using a cubic instead of a quadratic fit.

Figures 5-8 are energy distributions for various ion species obtained from Si-doped GaAs. These are energy distributions obtained by a retarding potential method, i.e. by varying the sample potential while keeping the energy analyzer and extraction potential fixed. In all cases, ion energy increases to the left. Zero ion energy is where the ion intensity begins to increase abruptly. In figures 5 and 6, the energy distributions are shifted because of specimen charging (due to a Schottky barrier contact between the specimen and specimen mount). Similar distributions, obtained where charging effects are eliminated (by illuminating the specimen) are shown in Figures 7 and 8.

We found that for a specimen of GaAs that exhibited charging effects dependent on the intensity of light from the illuminator, the charging effects disappeared when the beam sputtered all the way through the specimen. This evidently converted the Schottky barrier to an ohmic contact because there were no charging effects subsequently no matter where the beam impinged on the sample.

Regarding Figures 5 and 6, it will be noted that there is a significant ion intensity on the right of the "normal energy distribution". This is due to ions generated in the gas phase. The case of mass 28 is particularly noteworthy. The gas phase ions (^{28}CO or $^{28}\text{N}_2$) result in ions that apparently have less than zero energy (these are ions that have not experienced the full accelerating potential, hence are evidently produced in the space above the specimen).

The very narrow energy distribution of ^{28}Si ions in Figures 5 and 7 is also noteworthy. It seems to indicate a different mechanism of ion production than the usual case (perhaps resonance ionization due to excited states of the emitted ion).

3.0 Summary

The present work has clarified some of the ambiguities in the literature concerning thermal conversion of GaAs. This work which is described in greater detail in a paper to be published in J. Appl. Phys. (refer to Appendix A) indicates that the 1.407 eV emission peak is probably due to a $\text{Si}_{\text{As}}\text{-V}_{\text{As}}$ complex and not to recombination at Mn impurities. It also indicates that the 1.363 eV peak may be due to recombination involving a $\text{Si}_{\text{As}}\text{-V}_{\text{Ga}}$ complex and not to Cu contamination. This 1.363 eV peak has been correlated with the thermal conversion effect by comparing its intensity with the resistivity of the thermally converted layer. In all cases of thermally-converted specimens, a depletion of Cr in a layer 1-2 μm thick was observed by SIMS.

The improvements of the QMAS instrument and computer programs for data acquisition indicate that it will be a powerful tool not only for further investigations of the type described in the present investigations but also in other on-going by DoD agencies at USC. These investi-

gations include studies of depth profiles of MBE grown materials and of ion implanted materials, studies of impurity concentrations in bulk materials and studies of photoconductivity in semiconductors.

4.0 Acknowledgements

The following researchers at USC have contributed to the work described in this report or publications resulting from this work:

Li-Hen Chang (Graduate student in Computer Science)

F. D. Guo (Graduate student in Electrical Engineering)

M. Huang (Graduate student in Computer Science)

S. Y. Yin (Graduate student in Materials Science - PhD, Jan. 1983)

M. Kotera (Post-doctoral fellow) not supported by this grant.

R. L. Lisiecki (Undergraduate & graduate student in EE; BS, January 1982) not supported by this grant

R. A. Wittry (Former undergraduate student in EE; BS, January 1980) not supported by this grant.

Additional contributions by researchers at NOSC and Hughes Research Laboratories are acknowledged in the publications listed in Appendix A.

Appendix A - Bibliography of Publications

"Use of Cathodoluminescence and SIMS in the Study of Thermal Conversion of GaAs", with S.Y. Yin, Microbeam Analysis - 1982, K.F.J. Heinrich, ed., San Francisco Press, 1982, pp. 413-14.

"Study of the Thermal Conversion of Semi-Insulating GaAs:Cr with Cathodoluminescence, Photoluminescence and Secondary Ion Mass Spectrometry", with S.Y. Yin, accepted by J. Applied Physics (scheduled for Jan. 1983).

"Gaussian Models for the Energy Distribution of Excitation in Solids: Applications to Solid State Electronics", in Electron Beam Interactions in Solids to be published by SEM Inc. (in press).

Appendix B - Figures showing QMAS Results

List of Figures

- Fig. 1 Depth profile of a superlattice of Si and Si-7.5%Ge
- Fig. 2 Depth profile of Si implanted in GaAs with implantation energy of 100 keV and fluence of 4×10^{15} ions/cm³
- Fig. 3 Histogram mass spectrum of Czochralski-grown Si
- Fig. 4 Histogram mass spectrum of GaAs
- Fig. 5 Energy distribution of some ion species from GaAs when charging effects are present.
- Fig. 6 Energy distribution of additional ion species from GaAs when charging effects are present.
- Fig. 7 Energy distribution of some ion species from GaAs when charging effects are absent.
- Fig. 8 Energy distribution of additional ion species from GaAs when charging effects are absent.

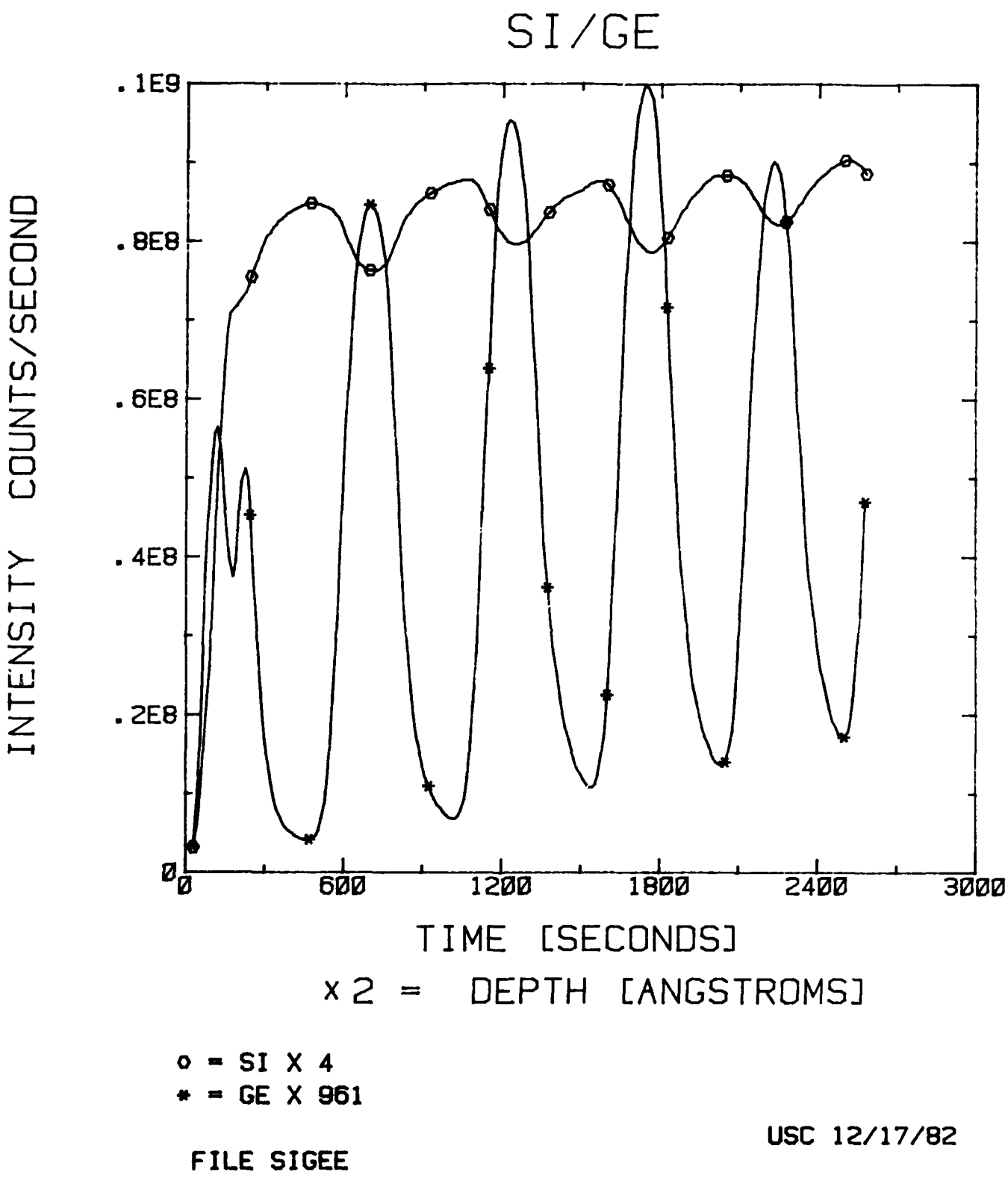
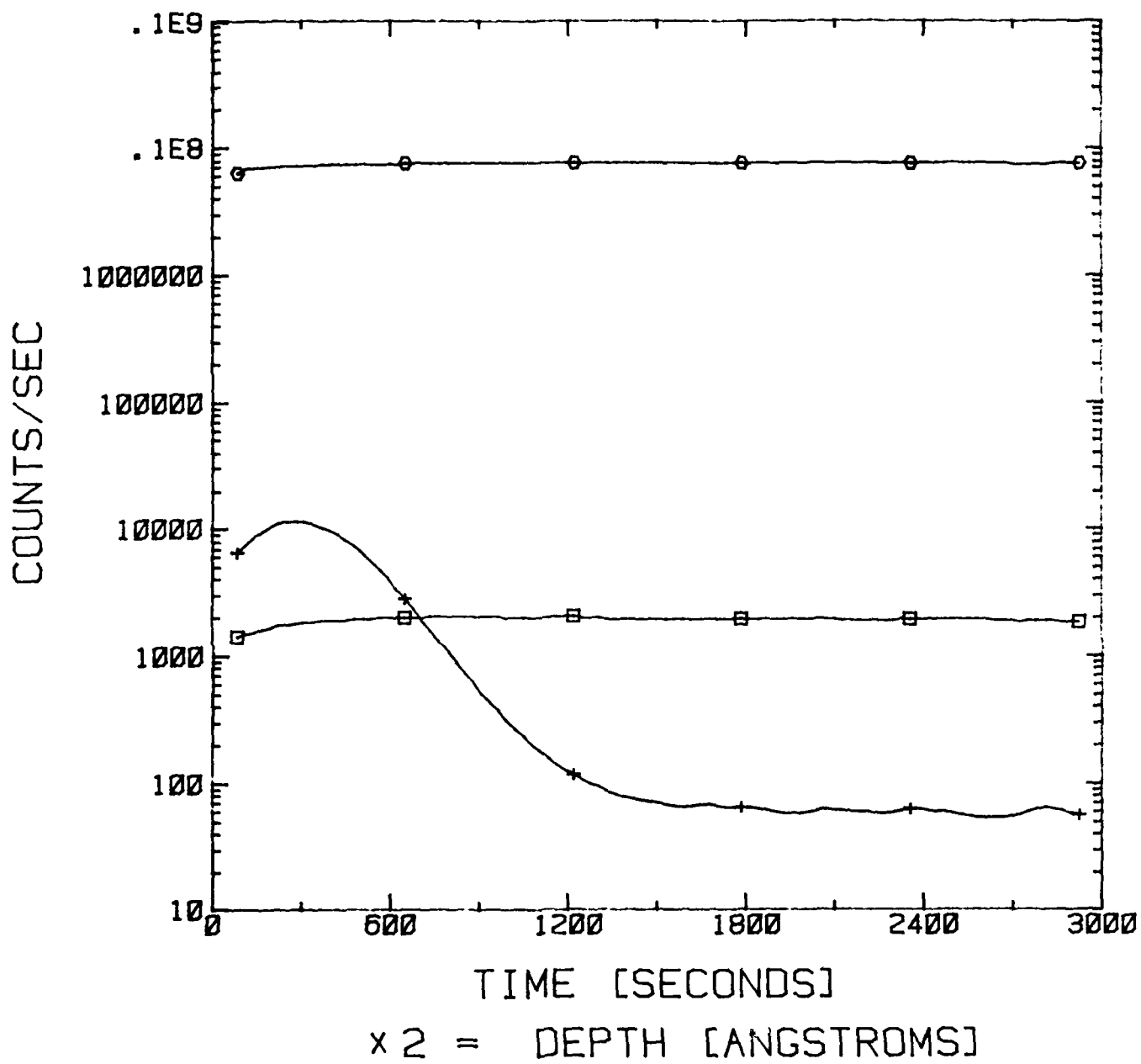


Fig. 1

GAAS(SI)



○ = GA

□ = AS

+ = SI

USC 12/26/82

FILE INPLD

Fig. 2

CZ-SI SPECTRUM # 2

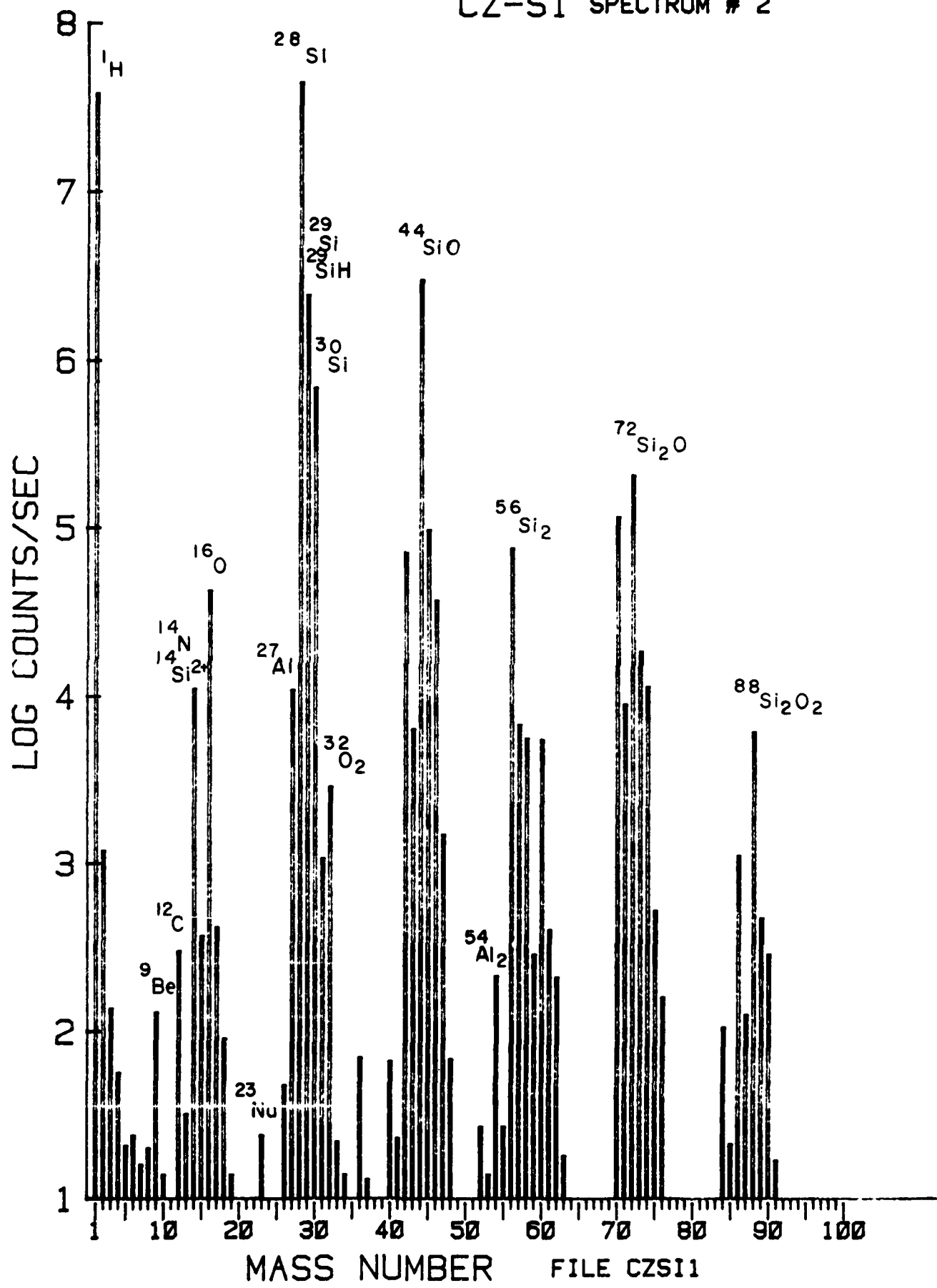


Fig. 3

FILE CZSII

USC 12/30/82

GAAS SPECTRUM # 2

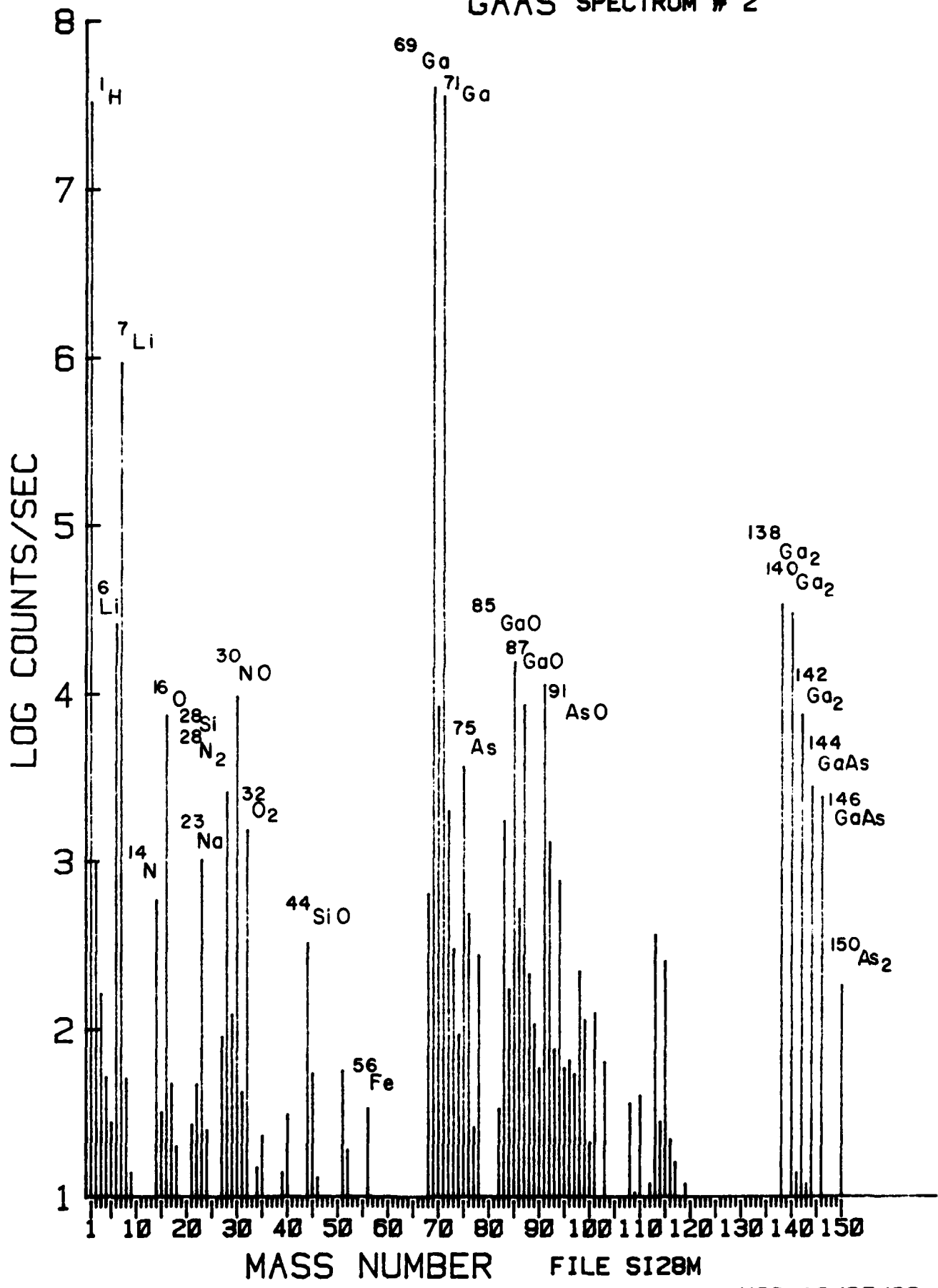
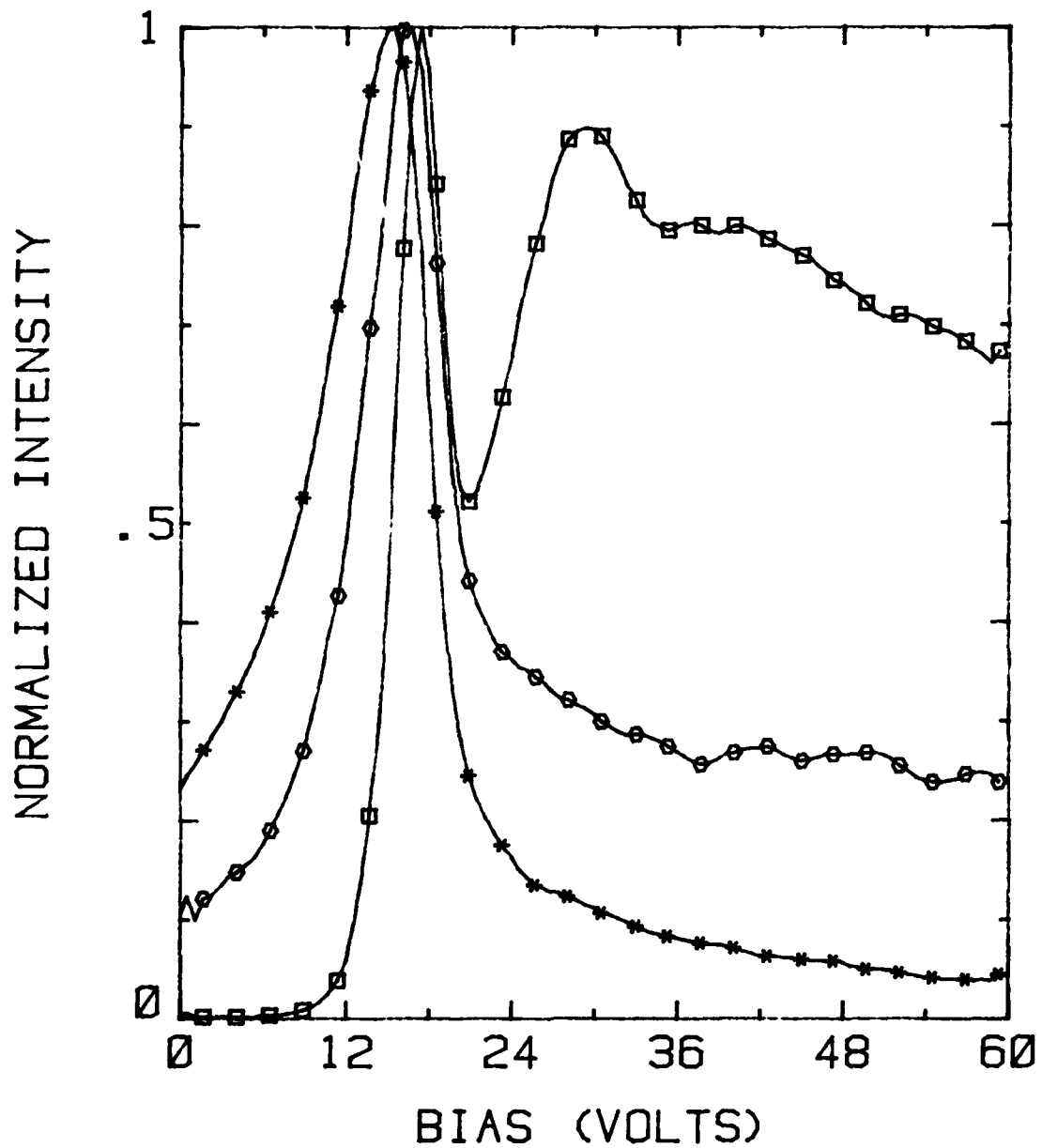


Fig. 4

EGAI6

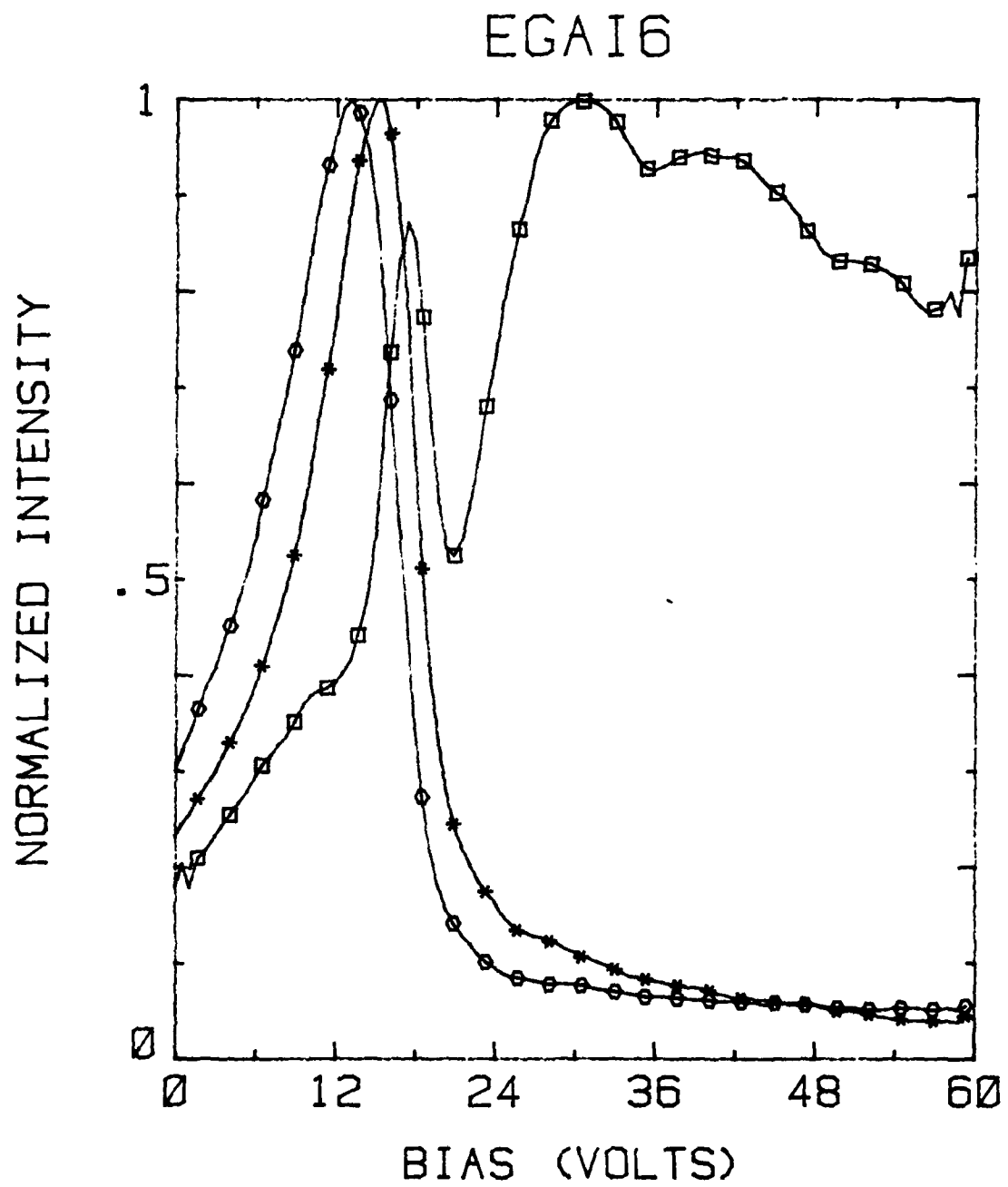


○ = N X3.231
□ = Si+N₂ X1
* = As X1.022

USC 12/30/82

FILE EGAI6

Fig. 5

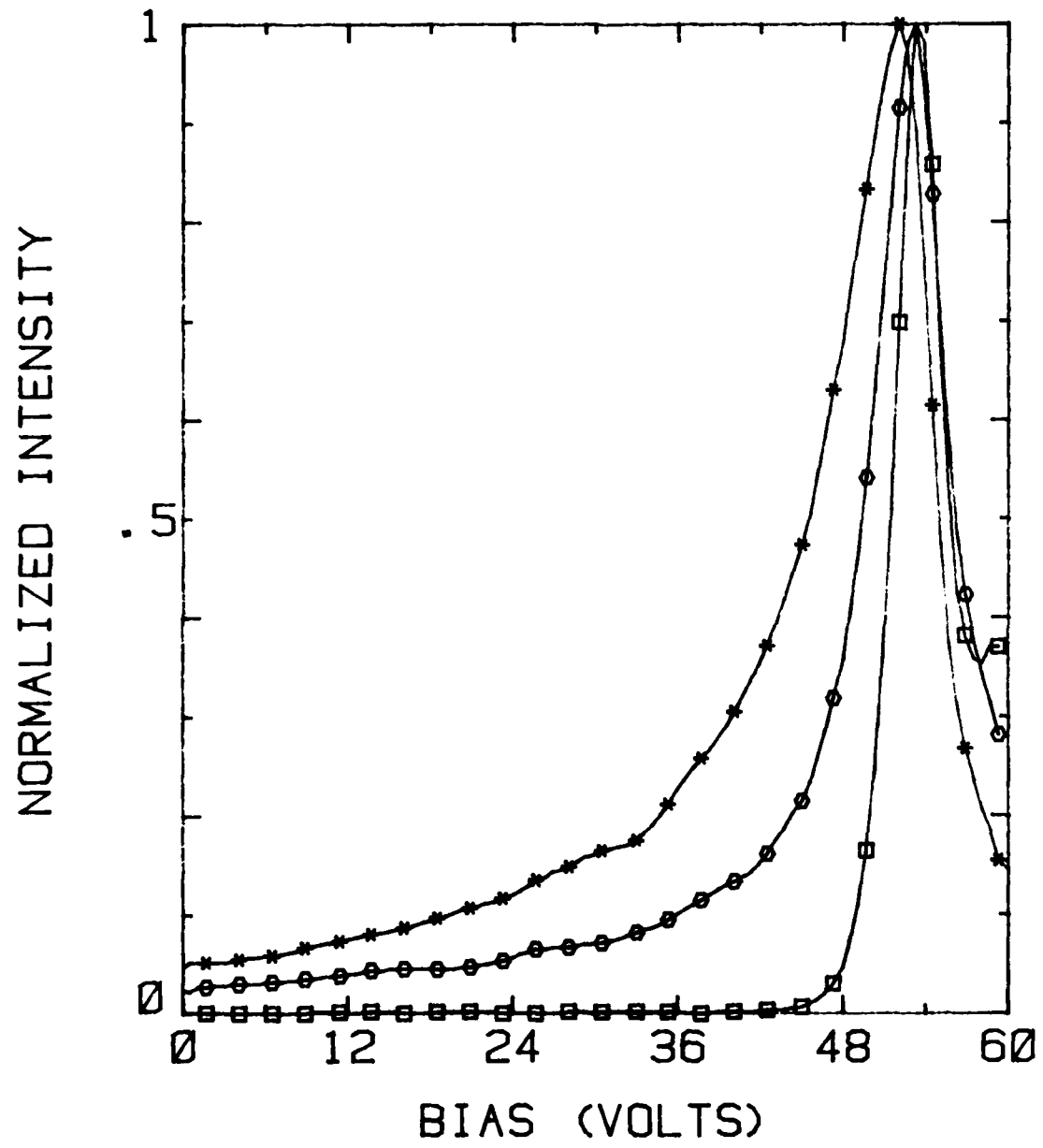


USC 12/30/82

FILE EGAI6

Fig. 6

EGA I4



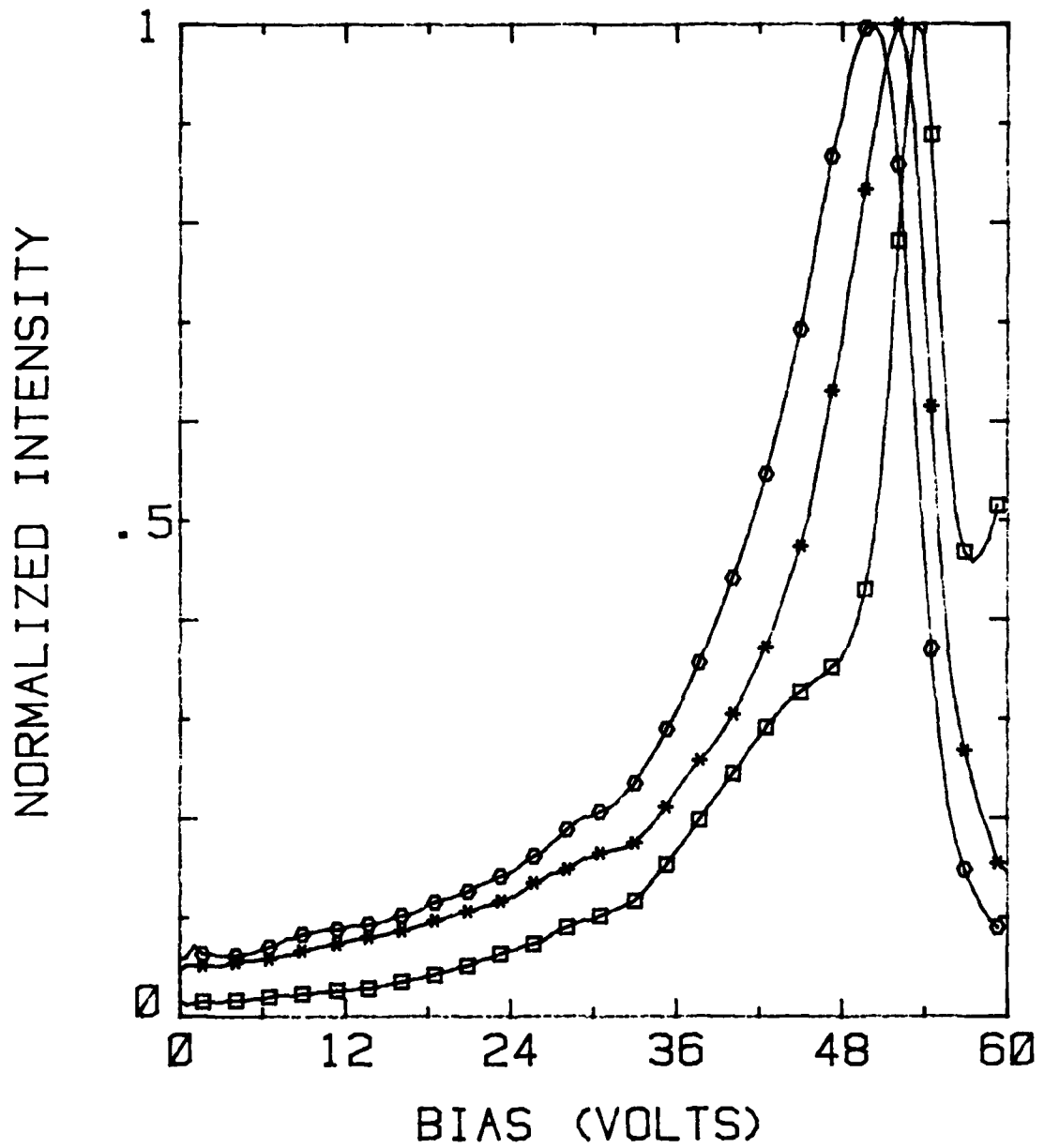
○ = N X3.445
□ = Si+N₂ X1
★ = As X1.298

USC 12/30/82

FILE EGAI4

Fig. 7

EGA I4



○ = O X1.006
□ = O₂ X1.878
* = As X1

USC 12/30/82

FILE EGAI4

Fig. 8

END
DATE
FILMED

5 -83

DTIC